Vol. 25, No. 2(2026) IA26786

Revista Mexicana de Ingeniería Química

Application of Electro-Fenton methods in the remediation of the Nexapa River

Aplicación de métodos Electro-Fenton en el saneamiento del río Nexapa

N.J. Camarón-Morales[1], M. A. Pérez-Cruz[1], M. Sánchez-Cruz[1], E. Aguilar-García[2], R. Torralba-Sánchez[3], G. Vidal-García[4,5], M. P. González-Aráoz[4], D. J. Caballero-Jiménez[1*]

[1] Facultad de Ciencias Químicas, Benemérita Universidad Autónoma de Puebla, 18 Sur y Avenida San Claudio, Ciudad Universitaria, Puebla, México, C.P. 72570.

[2] Escuela Superior de Física y Matemáticas, Instituto Politécnico Nacional, Av. Instituto Politécnico Nacional s/n, Unidad Profesional "Adolfo López Mateos", Colonia San Pedro Zacatenco, Gustavo A. Madero, Ciudad de México, México, C.P. 07738.

[3] Complejo Regional Mixteca, Campus Izúcar de Matamoros 141, Benemérita Universidad Autónoma de Puebla, Carr. Atlixco-Izúcar de Matamoros 141, San Martín Alchichica, Izúcar de Matamoros 74750, Puebla, Mexico.

[4] Facultad de Ingeniería, Benemérita Universidad Autónoma de Puebla, 16 Sur y Avenida San Claudio, Ciudad Universitaria, Puebla, México, C.P. 72570.

[5] Departamento de Materiales, Universidad Autónoma Metropolitana-Azcapotzalco, Av. San Pablo 180 Col. Reynosa-Tamaulipas, C.P. 02200, CDMX, México.

Received: February 3, 2026; Accepted: May 6, 2026

Abstract

This research evaluates the effectiveness of the Electro-Fenton (EF) treatment in removing contaminants from water samples collected from the Nexapa River in Puebla, Mexico. Previous studies in the area reported elevated levels of Chemical Oxygen Demand (COD), as well as Cr and As levels exceeding the limits set by Mexican Official Standards. A series of EF experiments were performed in electrolytic cells by varying the applied voltage, treatment time, and H_2O_2 dosage to identify the optimal conditions for removing contaminants. Optimal operating conditions of 9 V for 5 min with 0.05 mL of H_2O_2 led to a COD reduction of up to 93.5% and decreases of 62.5% and 93.53% in Cr and As concentrations, respectively. UV–Vis analysis proved to be a reliable tool for monitoring the progressive elimination of organic compounds, showing a direct relationship with the COD values. The reductions in total Cr and As levels were determined using atomic absorption spectroscopy (AAS). Gravimetric analysis established the optimal treatment ratio for [COD]:[Fe^{2+}]:[H_2O_2] at 1:2.4:0.85 ppm. The experiments were performed under batch conditions, and the results confirm the efficiency of the EF process for treating contaminated water in this region and provide a solid preliminary basis for further studies aimed at designing an efficient and sustainable treatment alternative.

Keywords: advanced oxidation processes, electrochemistry, Electro-Fenton, water pollution.

Resumen

Esta investigación evalúa la eficacia del tratamiento Electro-Fenton (EF) para la remoción de contaminantes en muestras de agua recolectadas del río Nexapa, en Puebla, México. Estudios previos en la zona reportaron niveles elevados de Demanda Química de Oxígeno, así como concentraciones de Cr y As que exceden los límites establecidos por las Normas Oficiales Mexicanas. Se llevó a cabo una serie de experimentos de EF en celdas electrolíticas, variando el voltaje, el tiempo de tratamiento y la dosificación de H_2O_2, con el fin de identificar las condiciones óptimas para la remoción de contaminantes. Las condiciones óptimas de operación a 9 V durante 5 min con 0.05 mL de H_2O_2 permitieron alcanzar una reducción del DQO del 93.5%, así como disminuciones del 62.5% y del 93.53% en las concentraciones de Cr y As, respectivamente. Los análisis por UV–Vis se usaron para monitorear la eliminación de compuestos orgánicos, mostrando una relación directa con los valores de DQO. La reducción de los niveles totales de Cr y As se determinó mediante espectroscopía de absorción atómica. Un análisis gravimétrico estableció la relación óptima de tratamiento [DQO]:[Fe^{2+}]:[H_2O_2] de 1:2.4:0.85 ppm. Los experimentos se llevaron a cabo en condiciones discontinuas, y los resultados confirman la eficacia del proceso EF para el tratamiento del agua contaminada en esta región y proporcionan una base preliminar sólida para futuros estudios destinados a diseñar una alternativa de tratamiento eficiente y sostenible.

Palabras clave: procesos de oxidación avanzada, electroquímica, Electro-Fenton, contaminación del agua.

* *Corresponding author. E-mail*: judith.caballerojim@gmail.com ;

https://doi.org/10.24275/rmiq/IA26786

ISSN:1665-2738, *issn-e*: 2395-8472

1 Introduction

It is estimated that between 85% and 90% of wastewater worldwide is discharged directly into rivers, lakes, and oceans (World Health Organization [WHO], 2017). Currently, this problem is a priority on the global environmental agenda, as its consequences affect both aquatic ecosystems and public health. In addition, rapid global population growth has increased the water demand for agricultural, industrial, and domestic activities, leading to an unprecedented global water crisis (United Nations Educational, Scientific and Cultural Organization [UNESCO], 2015).

Given this alarming situation, it is crucial to develop sustainable, efficient, and large-scale wastewater treatment methods that do not compromise ecosystem integrity or adversely affect the surrounding communities. The Advanced Oxidation Processes (AOPs), and particularly the Electro-Fenton (EF) process (Fenton, 1884), are considered among the most promising technologies (Vázquez Romero *et al*., 2024; Brillas, Sirés, & Oturan, 2009; Medrano-Hurtado *et al*., 2024). In the EF process, H_2O_2 reacts with ions Fe^{2+} ions in an acidic medium, generating highly reactive ·OH radicals. The continuous regeneration of Fe^{2+} from Fe^{3+} ions through redox reactions sustains the catalytic cycle; while the ·OH radicals act as powerful, non-selective oxidizing species that attack organic matter, promoting its degradation into intermediate compounds such as alcohols, carboxylic acids, and aldehydes. With continued oxidation, these intermediates are transformed in simple inorganic compounds such as CO_2 and H_2O. This process is illustrated in Scheme 1 (Ribeiro & Nunes, 2021; Ziembowicz & Kida, 2022; Lin *et al*., 2025).

$$Fe^{2+} + H_2O_2 \rightarrow Fe^{3+} + OH^- + OH^{\cdot}$$
$$RH + HO^{\cdot} \rightarrow R^{\cdot} + H_2O$$
$$R^{\cdot} + Fe^{3+} \rightarrow R^+ + Fe^{2+}$$
$$Fe^{2+} + HO^{\cdot} \rightarrow Fe^{3+} + OH^-$$

Scheme 1. Electro-Fenton process, where RH represents organic matter (Ribeiro & Nunes, 2021).

Among the advantages of this method, it has been reported that hazardous reagents are not required, and high contaminant removal efficiencies can be achieved with a relatively simple, low-cost technology (Soto-Vázquez *et al*., 2023; Nidheesh *et al*., 2023; Quispe Cardenas *et al*., 2023). However, to achieve an efficient process, key operational parameters such as pH, type, size and distance of electrodes, H_2O_2 dosage and voltage used, among others, must be selected according the characteristics of the water sample (Sun *et al*, 2015). In particular, literature contains numerous studies on the effect of pH on the efficiency of the EF process. Most of the studies reported that the optimum pH of the EF process is around 3 for preventing the formation and precipitation of $Fe(OH)_3$, at higher pH values, while for pH values below 3, iron species form stable complexes with H_2O_2, leading to deactivation of the catalysts (Nidheesh & Gandhimathi, 2012; Neyens & Baeyens, 2003).

On the other hand, widespread pollution across the 18-hydrological region has been documented in recent decades. This region corresponds to the Balsas River, located in the Mixteca region of southern Puebla, Mexico, and is recognized as one of the most important areas for its biological, cultural, and economic diversity. The Nexapa River is located within this region, near the municipality of Izúcar de Matamoros, with approximately 542,000 inhabitants. Currently, environmental degradation has led to accelerated biodiversity loss, the destruction of natural habitats, and adverse effects on natural resource regeneration processes and on the public health of communities along the river (Silva Gómez *et al*., 2002). Recent studies have reported the presence of emerging contaminants (ECs) and organic micropollutants (OMPs) in the Nexapa River. Most of these compounds are not effectively removed by conventional wastewater treatment systems and act as endocrine disruptors, mutagens, and even carcinogens, affecting aquatic organisms and humans. Research by Navarro *et al*, has identified at least 398 organic compounds in this river, including flavorings, food colorings, ketones, aldehydes, organic acids, and sulfur compounds. In addition, substances used in the formulation of industrial solvents, pesticides, products derived from plastics and chemical industries, short-chain aromatic hydrocarbons, and chlorinated phenols (intermediates in pesticide synthesis), as well as components of cleaning products, cosmetics, fragrances, sunscreens, and personal hygiene items, among many others, have been detected (Navarro, Herrera, Marrugo, Bayona, & Morales, 2014; Navarro-Frómeta *et al*., 2024). This wide range of compounds highlights the strong anthropogenic impact on the Nexapa River, particularly due to the uncontrolled discharge of domestic and industrial wastewater. In addition, heavy metals were detected in 2002, during water quality monitoring conducted in wells, springs, and surface runoff sites near the river, which revealed elevated concentrations of nitrites, Cd, and Pb exceeding the permissible limits established by the Mexican normativity (SEMARNAT, 2021; Domínguez-Montero *et al*., 2024). The samples taken directly from the river contained high concentrations of nitrites, methylene blue active substances, ammoniacal nitrogen, Cd, Cr, As, and Pb (Silva Gómez *et al*., 2002). The presence of

these toxic elements in groundwater sources suggests the possible infiltration of contaminants from the river into the aquifer, constituting a direct risk to the local drinking water supply. This contamination was attributed to daily human activities, inadequate solid waste management, extensive agricultural, livestock, metallurgical, and mining activities, as well as local tourism, which has expanded without adequate environmental planning (Olvera Bautista *et al*., 2021). These combined factors represent a serious threat to the health of nearby populations and to crop safety, as water from the Nexapa River is widely used for irrigation, leading to the incorporation of contaminants into soils and agricultural products.

In this study, water samples from the Nexapa River were treated via the EF process. The results showed the effective removal of both organic and inorganic contaminants using accessible materials and straightforward characterization techniques. Optimization experiments were conducted in electrochemical cells by systematically varying key operational parameters, including the applied voltage, treatment time, and H_2O_2 dosage. Water quality was verified using several indicators, including sedimentable solids, chemical oxygen demand (COD), UV–Vis absorbance, turbidity, pH, total hardness, apparent color, expressed as the spectral absorption coefficient (α), and electrical conductivity. In addition, total As and Cr concentrations were quantified via atomic absorption spectroscopy (AAS). Gravimetric analysis was employed to establish the optimal treatment ratio among COD, Fe^{2+} ion concentration, and H_2O_2 dosage. Overall, the results provide a comprehensive evaluation of the efficiency of the EF process in removing organic and inorganic matter from Nexapa River water, representing an initial step toward the development and implementation of continuous treatment systems.

2 Methods and materials

2.1 Sampling

For this study, the sampling point was strategically selected to reflect the direct influence of the nearest community, known as "La Galarza," on the water quality of the river. Five aliquots of 200 mL each were collected over five consecutive days at the same sampling point, located at the geographical coordinates 18°40'54.3" N, 98°26'14.6" W, as indicated in Figure 1. The individual samples were characterized separately to highlight variations between sampling days, and the results are presented in Table 1. Most parameters remained consistent; however, notable differences were observed in the concentrations of nitrates, sulfates, and phosphates.

Figure 1. Geographic location of the sampling point, marked in blue.

Sampling was conducted in April, based on previous studies in the area that reported seasonal variations in the river's physicochemical characteristics, identifying April as the month with the highest parameter values due to low rainfall and extreme temperatures (Silva Gómez *et al*., 2002). After collection, the samples were preserved at 5 °C until analysis. Each sample was analyzed by duplicate to ensure reproducibility, and the average results were taken for the final analysis. Finally, the simple collected samples were homogenized and combined to obtain 1 L of a composite sample.

2.2 Equipment and solutions

Deionized water was obtained from an ultrapure water purification system (Barnstead E-Pure^{TM}) with a conductivity of 18.2 MΩ·cm. A 12% (w/v) NaCl solution and a 1% (v/v) HNO_3 solution were prepared using analytical-grade reagents from J.T. Baker. H_2O_2 (30% w/w) was obtained from Fermont and used as received. Solutions of EDTA 0.001 M were prepared from $C_{10}H_{14}N_2O_8{\cdot}2Na{\cdot}2H_2O$ and standardized with 0.1 M $CaCO_3$ using NET(1%) as an indicator. A buffer at pH 10 (50 mL) was prepared using NH_4Cl (0.133 g) and NH_4OH (1.9 mL). pH measurements were taken using a Conductronic 120 pH meter. Turbidity was measured with a Vernier sensor calibrated with a standard 100 NTU solution. Conductivity was determined using a YSI 3200 conductivity meter calibrated with a 0.1 N KCl solution. IR spectra were recorded on a Scimitar FT-IR Digilab Fourier transform infrared spectrophotometer with KBr pellets. UV-Vis spectroscopy spectra and COD measurements were performed on a Hach DR 5000 UV-Vis spectrophotometer using distilled water as the blank. COD was determined using low-range

Table 1. Characterization of the simple water samples collected in the Nexapa River.

Sample Point	pH	T (°C)	Turbidity (NTU)	Chloride (ppm)	Sulfates (ppm)	Nitrates (ppm)	Phosphates (ppm)	Total Hardness $CaCO_3$ (mg/L)	Setteable solids (mL/10 mL)
S1	7.77	27	2	113.29	320	42	33.2	414.5	0
S2	7.77	27	29	113.29	90	78	8.2	414.5	0
S3	7.45	28	196	79.90	30	7	2.5	399.9	3.5
S4	7.92	27	8	105.52	120	19	4.8	436.5	0
S5	7.64	24	35	99.97	130	7	2.4	304.52	0

Hach-brand vials (3–150 ppm), with a 100 ppm KHP standard. Apparent color was evaluated using UV-Vis spectroscopy and expressed as the absorption coefficient $\alpha(\lambda)$, representing the absorption of light per unit optical path length at the selected wavelengths (λ = 436, 525, and 630 nm). Total As and Cr were determined using a GBC 932 atomic absorption spectrophotometer (Scientific Equipment Ltd), employing calibration curves obtained from 2-15 ppm standard solutions for Cr and 30–70 ppm for As.

2.3 *Pre-treatment*

A volume of 250 mL of the previously homogenized composite sample was subjected to a thermal treatment in acid media before the EF treatment. For this procedure, the pH of the initial sample was adjusted to a range of 2.8–3.5 using 1% HNO_3. The sample was then heated at 75 °C under continuous stirring at 100 rpm for 60 min. Upon completion, hot gravity filtration was performed using qualitative filter paper, and the sample was allowed to cool to room temperature. Any volume loss due to heating and filtration was compensated for with deionized water to preserve the original analyte concentrations.

Previous studies have reported that thermal pretreatment under acidic conditions promotes the breakdown of complex organic and inorganic compounds, thereby facilitating their subsequent degradation within the EF system. Additionally, this pretreatment enhances sludge dewaterability by degrading proteins and polysaccharides, which reduces water retention in the sludge. Acidification also induces changes in the interparticle interactions among sludge flocs and their constituents (Dewil *et al.*, 2005; Pilli *et al.*, 2015). To evaluate whether this effect occurs in the Nexapa River samples, experiments with and without the pretreatment were conducted under the optimized operating conditions (H_2O_2 dosage of 0.05 mL, applied voltage of 9 V, and treatment time of 5 min). In the experiments conducted without pretreatment, the COD value increased by 19.8 ppm (5.8%), and the time required for organic matter degradation was extended by approximately 10 minutes compared to the pretreated samples. These results indicate that, although the pretreatment step is not strictly essential, it significantly enhances the efficiency of the EF process by promoting faster and more effective degradation of organic matter.

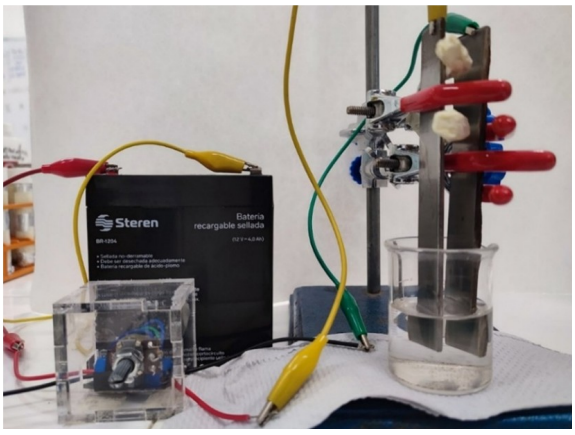

Figure 2. Configuration of the electrochemical cell.

2.4 *Electrolytical cells*

For the EF treatment stage, 45 mL of the previously digested sample was combined with 5 mL of a 12% NaCl solution as a supporting electrolyte, along with variable volumes of 30% H_2O_2 ranging from 0.01–1 mL. The electrochemical cells were assembled using two AISI 304 stainless steel electrodes, previously polished, to remove surface impurities and enhance electrical conductivity. The electrodes were positioned at a fixed interelectrode distance of 2.5 cm and an immersion depth of 2 cm, and were connected to a 12 V, 4 A rechargeable battery coupled to a voltage regulator. Applied voltages from 2 to 10 V and treatment times from 5 to 20 min were systematically evaluated to determine the optimal reaction conditions, as illustrated in Figure 2.

The efficiency of the electrochemical treatment was evaluated through the quantification of some of the main parameters established in the NOM-001-SEMARNAT-2021 standard for surface water bodies such as rivers, streams, and channels, in Mexico (Domínguez-Montero *et al.*, 2024). In addition, a gravimetric analysis was performed to determine the amount of Fe^{2+} released from the sacrificial electrode, with the objective of determining a stoichiometric relationship between the oxidizing agent concentration (H_2O_2) and the COD. All the analyses were replicated, and the average results were reported.

Table 2. Characterization of the composite water sample at 25 °C before the EF treatment.

Settleable solids (mL/10 mL)	pH	Total Hardness $CaCO_3$ (mg/L)	Turbidity (NTU)	α (m^{-1}) λ_1=436 nm λ_2=525 nm λ_3=620 nm	COD (ppm)	[Cr] (ppm)	[As] (ppm)
< 0.1	8.5 ±0.14	444.4 ± 23.7	31.5 ± 0.71	4.2 ± 0.01 2.5 ± 0.02 2.0 ± 0.01	340 ± 21.21	2.231 ± 0.05	11.063 ± 0.05

3 Results and discussion

According to the literature, the EF process can be classified into four groups. In the first one, Fe^{2+} and H_2O_2 are produced electrochemically at the surfaces of the sacrificial anode and the cathode, respectively. In the second type, known as the electrochemical peroxidation process, H_2O_2 is manually added to the reactor, while a sacrificial iron anode serves as the source of Fe^{2+}. In the third type, ferrous iron is added to the reactor, and H_2O_2 is produced through the diffusion of O_2 on the surface of the carbon cathode. In the fourth type, both Fenton reagents (H_2O_2 and Fe^{2+}) are added externally to the reaction medium (Sarabi *et al*., 2024). In the first and second types of EF processes, the iron required for the EF process was supplied by the oxidation of the used iron electrode. Aaron *et al*. reported that an increase in iron production in the treated results in an increase in the efficiency of the contaminant removal (Aaron *et al*., 2001). Some studies have demonstrated that the electrochemical peroxidation process offers significant advantages, including a reduced reliance on external iron salts and a continuous supply of Fe^{2+}. This is because the required Fe^{2+} is generated *in situ* via the oxidative dissolution of the sacrificial iron electrode, thereby enabling a more cost-effective process (Sarabi *et al*., 2024). For this reason, stainless steel sacrificial electrodes were selected for the experiments.

An aliquot of water from the composite sample was characterized before the electrochemical treatment (Table 2). Overall, the results indicate a markedly deteriorated water quality, as most of the analyzed parameters exceeded the limits established by current Mexican regulations. In particular, the COD values were consistent with those reported in recent studies, ranging from 221 to 382 mg/L at different sampling sites along the river, which classifies the water as heavily polluted due to exceeding the maximum permissible limit of 210 mg/L (Navarro-Frómeta *et al*., 2025; Arroyo Ortega *et al*., 2025).

In addition, total arsenic (As) and chromium (Cr) concentrations were detected at levels considered extremely hazardous to human health. According to official Mexican standards, the permissible limits for discharges into surface water bodies are 0.4 mg/L for As and 1.5 mg/L for Cr; however, the concentrations measured in the analyzed samples exceeded these thresholds by up to twenty-threefold for As and threefold for Cr.

Complementary optical parameters, including turbidity and apparent color, were also evaluated as indirect indicators of particulate and chromophoric matter, despite the absence of specific regulatory limits for surface waters. The turbidity of the composite sample indicated a substantial presence of suspended particles, which can interfere with light transmission and affect the optical response of the water matrix. The α values indicated a moderate level of apparent color in the analyzed water sample. The observed decrease in α with increasing wavelength ($\alpha_{436} > \alpha_{525} > \alpha_{620}$) is characteristic of waters containing dissolved organic matter, particularly aromatic and humic-like compounds that preferentially absorb light in the shorter wavelength region. These optical properties are consistent with the relatively high turbidity value and elevated COD, suggesting that both suspended particles and organic constituents contribute to the measured color (Helms *et al*, 2008).

The findings in Table 2 are consistent with previous studies in the region reporting high concentrations of organic matter and heavy metals (Navarro *et al*., 2013; Navarro-Frómeta *et al*., 2020; Navarro-Frómeta *et al*., 2024). The turbidity results indicate the presence of a significant fraction of suspended and colloidal particles in the water matrix, even though settleable solids were negligible. This suggests that particulate matter was mainly composed of fine particles that remain in suspension and can strongly influence the optical properties of the water. Apparent color, expressed as the absorption coefficient α, exhibited a decreasing trend with increasing wavelength, which is characteristic of waters containing chromophoric organic matter. Since apparent color integrates contributions from both dissolved compounds and suspended particles, the combined analysis of turbidity and α indicates that the observed coloration results from the simultaneous presence of particulate material and dissolved organic species. This optical behavior is consistent with the elevated organic load inferred from the physicochemical characterization of the sample. On the basis of these results, electrochemical experiments were conducted using 45 mL of sample, previously acid-digested, to evaluate the effects of voltage, treatment time, and H_2O_2 dosage. The results are presented below.

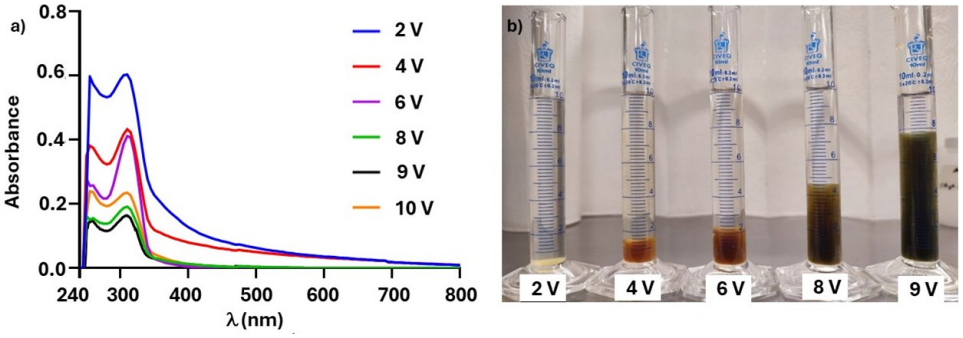

Figure 3. a) UV–Vis spectra and b) settleable solids obtained from voltage-variation experiments with 5 min of EF treatment.

Table 3. Influence of the voltage variation on the EF process at 25 °C and 5 min.

Voltage (V)	Settleable solids (mL/10 mL)	pH	Total Hardness $CaCO_3$ (mg/L)	Turbidity (NTU)	$\alpha(m^{-1})$ λ=436 nm	$\alpha(m^{-1})$ λ=525 nm	$\alpha(m^{-1})$ λ=620 nm
Untreated Sample	< 0.1	8.53 ± 0	444.4 ± 0	31.5 ± 0	4.2	2.5	2.0
2	<0.1	7.80 ± 0	37.33 ± 0.20	54.7 ± 0	9.2	5.4	3.3
4	1.4 ± 0.28	8.06 ± 0.01	34.46 ± 0.24	33.6 ± 0.28	6.5	4.5	3
6	2 ± 0.14	7.91 ± 0.01	33.53 ± 0.48	25.5 ± 0.14	0	0	0
8	4.4 ± 0	8.06 ± 0	30.06 ± 0.24	20.2 ± 0.28	0.7	0.3	0
9	7.1 ± 0.14	8.03 ± 0.03	25.40 ± 0.42	20.1 ± 0.70	0.4	0	0
10	7.6 ± 0.28	8.01 ± 0.14	23.40 ± 0.24	22.5 ± 2.80	0.5	0	0

3.1 Voltage variation

The optimal voltage for carrying out the electrochemical water treatment was determined by fixing the reaction time at 5 min and the H_2O_2 volume at 0.5 mL, while applying the following voltage values: 2, 4, 5, 8, 9, and 10 V. Subsequently, the main physicochemical parameters were evaluated to assess the quality of the treated water by comparing the results obtained at each voltage with those corresponding to the untreated sample. The influence of the applied voltage on the efficiency of the contaminant removal process is shown in Table 3.

As observed in the obtained results, the untreated sample exhibited a slightly alkaline pH (pH = 8.53). It has been reported that the pH is one of the most critical parameters affecting the EF process, and the optimal pH for conventional homogeneous EF systems typically ranges from 2.8 to 3.5, where Fe^{2+} solubility and the production of ·OH is maximized. This value can be difficult to achieve due to high chloride concentrations, which can alter pH through side reactions, and because some complex organic pollutants may act as buffers, complicating pH control. In addition, Fe^{3+} precipitates as iron sludge, thereby decreasing catalytic efficiency at pH > 4 (Ding *et al*., 2025). For this system, the use of a thermal treatment in acid media involves the use of HNO_3, reducing the pH to values close to 4. Then, the pre-treatment facilitates the initiation of the electrochemical treatment, and the cathodic reactions promote the generation of hydroxyl ions, leading to a progressive increase in pH and the restoration of alkaline conditions with values close to 8. The alkaline environment favored the subsequent formation of metal hydroxides in the solution. This pH behavior was independent of the applied voltage within the range of 2 to 10 V, which may be attributed to the achievement of a limiting concentration of hydroxyl species and metal hydroxide precipitates in the system.

The pH value has been suggested as a general reference parameter for system behavior; however, the observed voltage-independent values indicate that pH does not constitute a direct indicator of contaminant removal efficiency. Since COD determination represents a more expensive and time-consuming characterization method, UV–Vis spectroscopy was selected as a qualitative monitoring technique to assess the presence of residual organic matter in the water. This technique was chosen for its operational simplicity, accessibility, and lower cost compared with other analytical methods, such as COD or TOC determination. Specifically, absorbance was measured at a maximum wavelength (λ_{max}) of 254 nm, a region of the electromagnetic spectrum commonly associated with the presence of organic compounds, particularly those containing aromatic structures (Ramos Ascue, 2018). The progressive decrease in UV–Vis absorbance observed during the treatment indicates a reduction in organic matter content. This behavior is attributed to the degradation of chromophoric organic compounds, including aromatic and conjugated structures that strongly absorb in

Table 4. Influence of the time variation results on the EF process at 25 °C and 9V.

Time (min)	Settleable solids (mL/10 mL)	pH	Total Hardness $CaCO_3$ (mg/L)	Turbidity (NTU)	$\alpha(m^{-1})$ λ=436 nm	$\alpha(m^{-1})$ λ=525 nm	$\alpha(m^{-1})$ λ=620 nm
Untreated sample	< 0.1	8.53	444.4	31.5	4.2	2.5	2.0
5	4.6 ± 0.14	5.05 ± 0.014	150.0 ± 18.38	23.8 ± 0	0.6	0.4	0.2
7	5.5 ± 0	6.53 ± 0	123.3 ± 17.11	22.8 ± 0.28	1.2	0.7	0.5
10	8.2 ± 0.28	7.30 ± 0.014	83.0 ± 21.49	21.6 ± 0.14	3.6	2.3	1.6
15	8.3 ± 0.14	8.44 ± 0	73.2 ± 4.24	22.5 ± 0.28	4.9	3.4	2.6
20	8.2 ± 0	11.4 ± 0.028	63.3 ± 2.54	21.3 ± 0.42	2.5	1.9	1.5

the UV and visible regions. As these structures are oxidized or broken down into simpler, less light-absorbing species, the overall absorbance of the water matrix decreases. Therefore, the attenuation of UV–Vis signals reflects not only a loss of color, but also a transformation and partial removal of organic matter, consistent with the action of oxidative processes on dissolved organic compounds. This approach has been applied in previous studies and is considered a reliable indirect indicator of the organic matter concentration in wastewater (Weishaar *et al*., 2003).

Figure 3a presents the UV–Vis absorbance spectra of samples treated at different voltages, showing that the lowest absorbance at 254 nm was achieved at 9 V. This behavior is consistent with the observed increase in settleable solids (Figure 3b) and with the improvement in other water quality parameters, including total hardness, turbidity, and the spectral absorption coefficient α (Table 3). Overall, the results indicate that 9 V is the optimal operating voltage for electrochemical treatment, as it yields the highest contaminant removal efficiency in the treated sample.

On the other hand, it has been reported that the dissolution of Fe-containing sacrificial electrodes leads to the production of *in situ* coagulants, in which hydroxyl ions are generated at the anode via reduction, whereas H_2 bubbles are produced at the cathode via oxidation, thereby assisting in driving the generated floc to the water surface. At low solution pH and oxygenated water, ferrous ions are easily transformed into ferric ions. Depending on the pH, the electrogenerated ferric ions undergo hydrolysis to form monomeric and polymeric species in solution, which have a strong tendency to polymerize. The primary complex formed is $Fe(OH)_3$, which remains in the aqueous solution as a gelatinous suspension, thereby assisting in the removal of wastewater contaminants by either electrostatic attraction or complexation phenomenon with subsequent coagulation (Das *et al*., 2022). The observation of suspended solids at the start of the experiment, which subsequently settle, suggests electrocoagulation processes (EC) as part of the overall mechanism.

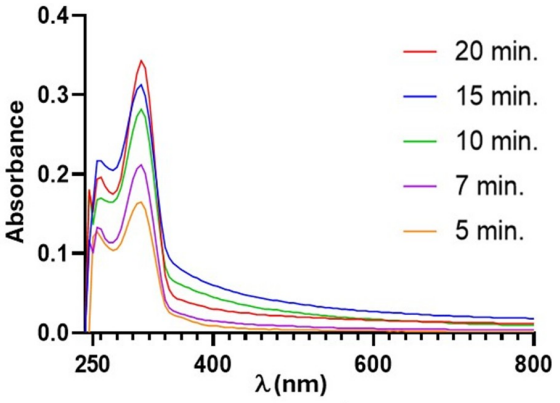

Figure 4. UV–Vis spectra at 25 °C with electrochemical cells at 9 V, 0.5 mL of H_2O_2, and time variation.

3.2 *Time variation*

Once the optimal voltage was established, additional experiments were conducted by varying the treatment time from 5 to 20 min. The objective was to identify the most efficient exposure time for the electrolytic treatment of contaminated water. Table 4 summarizes the detailed physicochemical characterization obtained for each evaluated treatment time.

Although the sample pH reached the value closest to neutrality (pH ≈ 8.2) after 10 min of treatment, the UV–Vis spectra recorded at λ = 254 nm (Figure 4) showed that the lowest absorbance was obtained after only 5 min. This result indicates that the most effective removal of organic matter occurred at shorter treatment times, suggesting that extended electrochemical exposure does not necessarily enhance contaminant degradation and may instead lead to secondary processes with a limited impact on organic matter removal.

To validate UV–Vis spectroscopy as a reliable and effective control parameter for monitoring organic matter removal during electrochemical treatment, colorimetric COD tests were conducted. The resulting data were used to construct absorbance versus treatment time plots based on the absorbance measured at the maximum wavelength (λ_{max}) of 254 nm (Figure 5a), as well as COD versus treatment

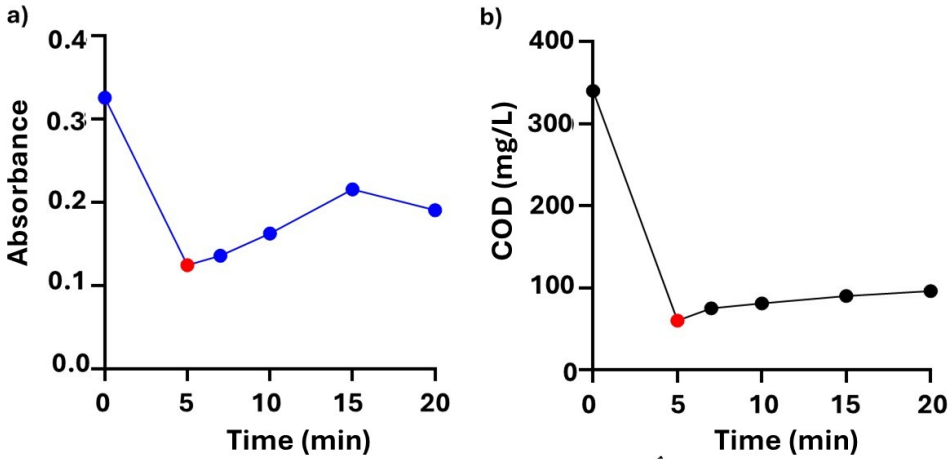

Figure 5. a) Absorbance vs t ratio obtained by UV-Vis, b) COD vs t ratio for electrochemical cells at 25 °C with 9 V, 0.5 mL of H_2O_2, and time variation treatment.

time plots (Figure 5b), allowing a direct comparison between both monitoring approaches.

Figure 5 shows that both parameters (UV–Vis absorbance and COD) exhibit similar trends, indicating a clear correlation between decreases in absorbance and COD. These results demonstrate that an optimal treatment time of 5 min is achieved when the electrochemical cell operates at 9 V with 0.5 mL of H_2O_2, and confirm that UV–Vis absorbance at λ_{max} = 264 nm is a reliable and effective parameter for monitoring organic matter removal.

As previously mentioned, earlier studies reported high concentrations of these metals in the Nexapa River water, consistent with the findings of the present study (Table 2). The measurements revealed that after 5 min of EF treatment at 9 V with 0.5 mL of H_2O_2, removal efficiencies of 29.8% for Cr and 39.47% for As were achieved. It has been documented that this decrease indicates that the mechanism of metal removal in the EF process does not involve mineralization, but rather the transfer of metallic species from the aqueous phase to the solid phase, mainly through coprecipitation and surface adsorption onto electrogenerated iron hydroxides (Yang *et al*., 2025). During this process, the anodic dissolution of iron leads to the continuous generation of Fe^{2+}/Fe^{3+} ions, which hydrolyze to form colloidal particles of $Fe(OH)_3$ and FeOOH. These highly reactive solid phases act as immobilization sites, where metal ions are removed by adsorption via inner-sphere complex formation and/or by coprecipitation within the iron hydroxide matrix.

When the treatment time was extended beyond 5 min, the Cr concentration increased, in some cases exceeding levels measured in the untreated water. This increase was attributed to the progressive degradation of the sacrificial electrodes used in the electrochemical cell, which are made of AISI 304 stainless steel containing approximately 18% of Cr. Other studies have observed the same process, in which chromium is released into the treated water; however, under treatment conditions, the form of chromium present is less toxic: Cr^{3+}. Furthermore, the chromium released by the process itself proves beneficial, as it acts as a catalyst, enhancing the generation of ·OH radicals and achieving bigger degradation of organic matter. A similar behavior was observed for total As, with metal concentrations returning to levels close to the initial values after 7 min of treatment. To remove these metals, post-treatment processes can be implemented, such as pH neutralization followed by filtration, adsorption, and coprecipitation. However, most of these metals are released after more than 5 minutes. Therefore, the optimal treatment time should not exceed this time, preventing the release of Cr and As (Li *et al*., 2026; Wu *et al*., 2024). This behavior, together with the observed increase in pH, suggests a restructuring of the solid phase, in which the electrogenerated hydroxides partially destabilize, thereby releasing metal ions back into the aqueous phase. This process may be further enhanced by strong desorption associated with changes in surface charge and the formation of soluble hydroxylated complexes, which are favored at higher pH values, thereby establishing a dynamic solid–liquid equilibrium. Therefore, precise control of the EF treatment time is essential not only to maximize organic matter removal but also to prevent the reintroduction of inorganic contaminants into the system.

On the other hand, numerous studies have demonstrated that fine-tuning the H_2O_2 concentration directly influences the rate of ·OH generation, thereby affecting both the degradation kinetics of organic matter and the removal behavior of metal ions. (Anotai *et al*., 2010; He & Zhou, 2017; Afolabi *et al*., 2022). Recently, Omar *et al*. employed an H_2O_2 dosage in range of 0.05–0.5 g/L for the treatment of

Table 5. Influence of the H_2O_2 dosage on the EF process at 25 °C, 9 V and 5 min.

H_2O_2 volume (mL)	Settleable solids (mL/10 mL)	pH	Total Hardness $CaCO_3$ (mg/L)	Turbidity (NTU)	α (m^{-1}) λ_1=436 nm λ_2=525 nm λ_3=620 nm	[Cr] (ppm)	[As] (ppm)	COD (ppm)
Untreated Sample	< 0.1	8.53	444.4	31.5	4.2 2.5 2.0	2.231	11.063	340
0.01	5.6 ± 0.14	6.20 ± 0	180 ± 28.28	1.5 ± 0.71	0.5 0.5 0.3	0.807 ± 0.81	0.843 ± 0.025	27 ± 7.07
0.05	6.4 ± 0	6.83 ± 0.03	160 ± 28.28	1.2 ± 0.28	0.5 0.5 0.3	0.836 ± 4.53	0.756 ± 0.022	22 ± 4.24
0.3	6.8 ± 0	6.45 ± 0.01	200 ± 42.42	1.5 ± 0.14	3.6 2.8 1.6	1.842 ± 1.84	5.687 ± 0.390	97 ± 11.3
1.0	3.6 ± 0.56	6.00 ± 0.01	600 ± 70.71	2.0 ± 1.41	4.9 3.4 2.6	> 15	8.786 ± 0.470	299 ± 7.07

industrial wastewater, concluding that excessive H_2O_2 acts as a scavenger of ·OH and reduces the process efficiency. Their results established an optimal dosage of 0.3 g/L (Omar *et al*., 2024). These findings are consistent with those reported by Delil and Gören, and Cheng *et al*., who achieved maximum COD removals of 76% and 89.8% using 250 and 300 mg/L of H_2O_2 for the treatment of sugar industry and petrochemical wastewater, respectively (Delil & Gören, 2019; Cheng *et al*., 2022). Similarly, Suhan *et al*. investigated the Fenton degradation of dyes in aqueous solution under optimal conditions, using 1000 mg/L H_2O_2 and achieving approximately 80% COD removal (Suhan *et al*., 2020). Overall, these results demonstrate that the optimal H_2O_2 dosage depends strongly on wastewater composition and must therefore be determined experimentally for each specific system.

Based on the prior studies, the effect of the H_2O_2 dosage (previously fixed at 0.5 mL) on the kinetics of the EF reactions was evaluated under the previously established optimal operating conditions (9 V and 5 min). A series of experiments was conducted by varying the H_2O_2 volume from 0.01 mL to 1 mL (66 – 6600 ppm), and the resulting kinetic response is summarized in Table 5.

As evidenced by the experimental results, reducing the volume of H_2O_2 used in the electrochemical treatment significantly enhances the removal efficiency of both organic and inorganic contaminants. In particular, a H_2O_2 volume of 0.05 mL (333.3 ppm) was identified as the optimal condition, achieving removal efficiencies of 62.5% for Cr, 93.16% for As, and 93.53% for COD relative to the initial concentrations. Regarding the remaining parameters, a 63.9% reduction in total hardness and an 88% decrease in color (λ_{max} = 436 nm) were observed, along with a substantial increase in settleable solids.

According to Gao *et al*., the produced sludge is a new type of complex, heterogeneous sludge composed of $Fe(OH)_3$, organic matter, heavy metals, microorganisms, sediment impurities, and moisture. Fenton sludge properties are largely dependent on the wastewater source and on the volume and ratio of the added reagents (Gao *et al*., 2022). The typical composition of the organic component of the sludge is composed of 7.36% carbon, 12.52% oxygen, 2.25% hydrogen, 0.78% nitrogen, and 0.85% sulfur. Only

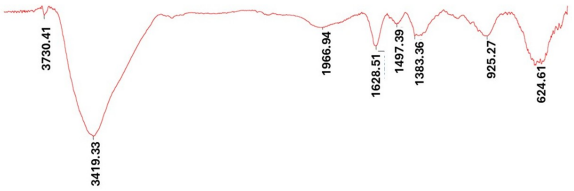

Figure 6. IR spectrum of the settleable solids generated during the EF treatment under optimal operating conditions.

a small part of the Fenton sludge contains solid matter, such that over 70% is water. Furthermore, Benatti *et al*. investigated the composition and metal content of Fenton sludge, and their results showed that the metals were present as amorphous materials, such as amorphous iron oxide (Benatti *et al*., 2006; Benatti *et al*., 2009). To verify if these characteristics are present in the sludge obtained for this research, properties such as pH, total chemical oxygen demand (TCOD), soluble chemical oxigen demand (SCOD),% of organic content, elemental analysis, and higher heating value (HHV), has been used in the other works for characterizing sludge in orden to find a suitable application for this material (Mahtab *et al*., 2021).

These solids were found to be insoluble across a wide range of solvents, including water, acetone, hexane, dimethyl sulfoxide (DMSO), ethanol, methanol, chloroform, dichloromethane, and toluene. The structural characterization of these solids was performed by infrared (IR) spectroscopy, and the resulting spectra are shown in Figure 6.

The FTIR spectrum reveals a broad band centered around 3419 cm^{-1} and another at 1628 cm^{-1}, which are associated with O–H stretching vibrations and the bending mode of adsorbed water, respectively. This result is consistent with the presence of structural water and/or surface hydroxyl groups in hydroxide and oxyhydroxide-type phases (Xu *et al*., 2022; De Jara *et al*., 2020; Cosme-Torres & Illescas-Martinez, 2025). Additionally, bands in the 1497–1383 cm^{-1} region were identified, which can be attributed to carbonate (CO_3^{2-}) vibrations or to simple oxygenated species adsorbed on the solid surface, possibly originating from interactions with atmospheric CO_2 or from byproducts of the electrochemical process. The signal observed around 925 cm^{-1} can be related to M–OH vibrations or out-of-plane deformations

of Fe–O–H bonds, which have been reported for poorly crystalline iron oxyhydroxides (Zhou *et al.*, 2012). The band at approximately 624 cm^{-1} is attributed to metal–oxygen (M–O) vibrations, which are commonly reported for inorganic materials based on metal oxides and hydroxides (Nakamoto, 2009; Socrates, 2004). The FTIR spectra of the solids obtained under different operating conditions are highly similar, suggesting that the solids are dominated by a comparable inorganic matrix (mainly iron hydroxides/oxyhydroxides) generated during the EF process. Complementary studies will be obtained in the next step of this work.

Conclusions

The performance of the electrochemical process was evaluated using parameters established by current Mexican regulations, specifically NOM-001-SEMARNAT-2021. Systematic variations in the operating conditions (applied voltage, treatment time, and H_2O_2 dosage) were conducted to assess their influence on process efficiency using composite water samples from the Nexapa River. This approach enabled the identification of optimal operating conditions that maximize contaminant removal efficiency.

The optimal operating conditions were identified at an H_2O_2 dosage of 0.05 mL, an applied voltage of 9 V, and a treatment time of 5 min. Under these conditions, organic matter removal reached 93.5%, as quantified by COD through colorimetric tests, together with substantial reductions in heavy metal concentrations of 63.8% for Cr and 93.53% for As, as determined by AAS. These results confirm the ability of the Electro-Fenton process to simultaneously remove organic and inorganic contaminants from the Nexapa River.

Process monitoring included pH evolution, which started in values close to 4, as a result of the previous thermal treatment in acid media, then increased during treatment due to electrogeneration of metal hydroxides and reached values close to neutrality under optimal operating conditions; however, pH changes alone were insufficient to track reaction progress accurately. In contrast, UV–Vis spectroscopy proved to be a more reliable monitoring approach, as absorbance measured at λ_{max} = 254 nm showed strong agreement with COD values and served as an effective indicator of organic matter degradation. In addition, H_2O_2 consumption was successfully monitored by following the absorbance band at λ_{max} = 240 nm, previously assigned to H_2O_2 (Hadwan *et al.*, 2024). Organic matter removal was primarily associated with the formation of settleable solids, whose FTIR characterization indicated that they were dominated by an inorganic matrix composed mainly of iron hydroxides/oxyhydroxides generated during the EF process.

Gravimetric analysis was used to quantify the amount of Fe^{2+} released by the corrosion of the sacrificial electrodes, which enabled the establishment of a stoichiometric relationship among [COD] : [Fe^{2+}] : [H_2O_2] of 1 : 2.4: 0.85 mg/L. This ratio proved optimal under the evaluated conditions and provides a quantitative basis for controlled dosing of H_2O_2 based on the initial COD of each sample, as well as on the Fe^{2+} concentration when inert electrodes are employed and an external metal salt is added. Consequently, these results provide a previous study for developing an understanding of the Nexapa River effluent.

Overall, these findings reinforce the viability of the electrochemical method as an efficient, cost-effective, and sustainable alternative for treating water from the Nexapa River contaminated with organic matter and heavy metals. Nevertheless, further studies are needed to evaluate process reproducibility, operational feasibility under continuous-flow conditions, and long-term economic performance under site-specific conditions. In addition, continued optimization of reagent ratios may further enhance treatment efficiency, reduce operational costs, and minimize the environmental impact associated with the implementation of this technology in the Nexapa River basin.

Acknowledgements

We thank the multidisciplinary group “Remediación Ambiental” from BUAP for providing the water samples used in this study.

ChatGPT (OpenAI) was used solely for language editing purposes. All scientific content, analysis, and conclusions are the responsibility of the authors.

References

Aaron, J. J., & Oturan, M. A. (2001). New photochemical and electrochemical methods for the degradation of pesticides in aqueous media. *Environmental Applications. Turk. J. Chem., 25(4),* 509–520. https://journals.tubitak.gov.tr/chem/vol25/iss4/15.

Afolabi, O. A., Adekalu, K. O., & Okunade, D. A. (2022). Electro-Fenton treatment process for brewery wastewater: Effects of oxidant concentration and reaction time on BOD and COD removal efficiency. *Journal of Engineering and Applied Science, 69(1)*, 42.

https://doi.org/10.1186/s44147-022-00089-1.

Anotai, J., Su, C. C., Tsai, Y. C., & Lu, M. C. (2010). Effect of hydrogen peroxide on aniline oxidation by electro-Fenton and fluidized-bed Fenton processes. *Journal of Hazardous Materials, 183(1–3)*, 888–893. https://doi.org/10.1016/j.jhazmat.2010.07.112.

Arroyo Ortega, I. F., García Zamora, J. L., Herrera Cárdenas, J. A., & Torres Ramírez, E. (2025). Herramientas SIG para la evaluación de la contaminación en el río Nexapa. *Revista MIX-TEC, 5(9),* 17–30. http://mixtec.utim.edu.mx/articulosv9/articulo02.pdf.

Benatti, C. T., Costa, A. C., & Tavares, C. R. (2009). Characterization of solids originating from the Fenton's process. *Journal of Hazardous Materials, 163(2–3),* 1246–1253. https://doi.org/10.1016/j.jhazmat.2008.07.094.

Benatti, C. T., Tavares, C. R., & Guedes, T. A. (2006). Optimization of Fenton's oxidation of chemical laboratory wastewaters using the response surface methodology. *Journal of Environmental Management, 80(1)*, 66–74. https://doi.org/10.1016/j.jenvman.2005.08.014.

Brillas, E., Sirés, I., & Oturan, M. A. (2009). Electro-Fenton process and related electrochemical technologies based on Fenton's reaction chemistry. *Chemical Reviews, 109(12)*, 6570–6631. https://doi.org/10.1021/cr900136g.

Cheng, S., Ran, X., Ren, G., Wei, Z., Wang, Z., Rao, T., Li, R., Ma, X. (2022). Comparison of Fenton and ozone oxidation for pretreatment of petrochemical wastewater: COD removal and biodegradability improvement mechanism. *Separations, 9(7)*, 179. https://doi.org/10.3390/separations9070179

Cosme-Torres, I, Illescas-Martínez, F. J. (2025). Heterogeneous photo-Fenton treatment in the degradation of indigo carmine (IC) by using ZeoSonFe as a catalyst through an experimental design. *Revista Mexicana de Ingeniería Química, 24(2)*, IA25520. https://doi.org/10.24275/rmiq/IA25520.

Das, P. P., Sharma, M., & Purkait, M. K. (2022). Recent progress on electrocoagulation process for wastewater treatment: A review. Separation and Purification Technology, *292*, 121058. https://doi.org/10.1016/j.seppur.2022.121058

De Jara, E. M., García-Hernández, E., Quequezana-Bedregal, M. J., Arrieta-González, C. D., Salgado-Delgado, R., Lastarria-Tapia, H., & Castañón-Vilca, J. A. (2020). Potato starch-based films: Effects of glycerol and montmorillonite nanoclay concentration. *Revista Mexicana de Ingeniería Química*, *19(2),* 627-637. https://doi.org/10.24275/rmiq/Bio823.

Delil, A.D. and Gören, N. (2019). Treatment of sugar industry wastewater with Fenton and electro-Fenton: Response surface methodology approach on Fenton process. Presentation. June 18. Istanbul, Turkey: 4th Eurasian Conference on Civil and Environmental Engineering (ECOCEE). https://www.researchgate.net/publication/334965681.

Dewil, R., Baeyens, J., & Neyens, E. (2005). Fenton peroxidation improves the drying performance of waste activated sludge. *Journal of Hazardous Materials, 117(2–3),* 161–170. https://doi.org/10.1016/j.jhazmat.2004.09.025.

Ding, H., Ma, Q., Zhang, X., Wang, C., You, N., & Deng, S. (2025). Material design and operation strategy of the electro-Fenton system for the treatment of high pollutant load wastewater. *Sustainability, 17*, 10501. https://doi.org/10.3390/su172310501

Domínguez-Montero, L. E., Poggi-Varaldo, H. M., Cañizares-Villanueva, R. O., Padilla-Viveros, A. A., Rinderknecht-Seijas, N., Caffarel-Méndez, S., & Cruz-Burelo, E. (2024). Regulaciones para la descarga de aguas residuales de México: Comparación con otros países y su cumplimiento en plantas de tratamiento seleccionadas. *Revista Internacional de Contaminación Ambiental, 40*, 289–311. https://doi.org/10.20937/RICA.54362.

Fenton, H. J. H. (1894). Oxidation of tartaric acid in presence of iron. *Journal of the Chemical Society, Transactions, 65*, 899–910. https://doi.org/10.1039/CT8946500899.

Gao, L., Cao, Y., Wang, L., & Li, S. (2022). A review on sustainable reuse applications of Fenton sludge during wastewater treatment. Frontiers of Environmental *Science & Engineering*, *16(6)*, 77. https://doi.org/10.1007/s11783-021-1511-6.

Hadwan, M. H., Hussein, M. J., Mohammed, R. M., Hadwan, A. M., Al-Kawaz, H. S., Al-Obaidy, S. S. M., & Al Talebi, Z. A. (2024). An improved method for measuring catalase

activity in biological samples. *Biology Methods and Protocols, 9(1),* bpae015. https://doi.org/10.1093/biomethods/bpae015.

He, H., & Zhou, Z. (2017). Electro-Fenton process for water and wastewater treatment. *Critical Reviews in Environmental Science and Technology, 47(21*), 2100–2131. https://doi.org/10.1080/10643389.2017.1405673.

Helms, J. R., Stubbins, A., Ritchie, J. D., Minor, E. C., Kieber, D. J., & Mopper, K. (2008). Absorption spectral slopes and slope ratios as indicators of molecular weight, source, and photobleaching of chromophoric dissolved organic matter. *Limnology and Oceanography*, *53(3)*, 955–969. https://doi.org/10.4319/lo.2008.53.3.0955.

Li, Y., Xie, S., Duan, Y., Qian, A., Yuan, S., Fortner, J. D., & Liao, P. (2026). Elucidating an unrecognized iron leaching mechanism via sequential reduction-oxidation of passivation layer on stainless-steel cathodes for electro-Fenton process. *Water Research*, 125617. https://doi.org/10.1016/j.watres.2026.125617.

Lin, Y., Qiao, J., Sun, Y., & Dong, H. (2025). The profound review of Fenton process: What's the next step? *Journal of Environmental Sciences, 147*, 114–130. https://doi.org/10.1016/j.jes.2023.10.005.

Mahtab, M. S., Farooqi, I. H., & Khursheed, A. (2021). Zero Fenton sludge discharge: A review on reuse approach during wastewater treatment by the advanced oxidation process. *International Journal of Environmental Science and Technology, 10*, 1–14. https://doi.org/10.1007/s13762-020-03121-0.

Medrano-Hurtado, Z. Y., Marcelo-Medrano, A., Jumilla-Corral, A. A., & Mayorga-Ortiz, P. (2024). Evaluation of an electrooxidation and UV system with solar energy for the treatment of washing machine greywater for toilet and urinal discharges. *Revista Mexicana de Ingeniería Química*, *23*, IA24341. https://doi.org/10.24275/rmiq/IA24341

Navarro, A., Herrera, J., Marrugo, J., Bayona, J., Morales, L. (2014). Microcontaminantes orgánicos en los ríos de México: El caso del río Nexapa. In: *Ciencias de la Ingeniería y Tecnología Handbook T-IV*, (M. Ramos and V. Aguilera, eds.), Pp. 49-63. ECORFAN Press, México.

Navarro, A., Herrera, J., Caso, L., & Marrugo, J. (2013). Calidad del agua del río Nexapa: Tendencias espacio-temporales y sus implicaciones. *In Handbook TI,* pp. *83–97.* ECORFAN Press, México.

Navarro-Frómeta, A.E., Navarrete-Rosas, D. (2020). Addressing stressors to riverine waters quality: The case of the Nexapa River. In: *Water Availability and Management in Mexico*, (E.M. Otazo-Sánchez, A. Navarro-Frómeta and V.P. Singh, eds.), Pp. 127-149. Springer, Cham. https://doi.org/10.1007/978-3-030-24962-5_6.

Navarro-Frómeta, A. E., Marrugo-Negrete, J. L., & Bayona-Termens, J. M. (2024). Presence of organic micropollutants in agricultural waters and soils. *Terra Latinoamericana, 42*, 1–15. https://doi.org/10.28940/terra.v42i0.1798.

Navarro-Frómeta, A. E., Crespo-Barrera, P. M., & Horta-Valerdi, G. M. (2025). Interbasin water transfer: The case of the Nexapa River, Mexico. *MOJ Ecology & Environmental Sciences, 10(1)*, 1–3. https://doi.org/10.15406/mojes.2025.10.00338.

Nakamoto, K. (2009*). Infrared and Raman spectra of inorganic and coordination compounds: Part A: Theory and applications in inorganic chemistry (6th ed.).* Editorial John Wiley & Sons, New Jersey, E.U. https://doi.org/10.1002/9780470405840.

Neyens, E., Baeyens, J. (2003). A review of classic Fenton?s peroxidation as an advanced oxidation technique. *Journal of Hazardous Materials 98(1-3)*, 33-50. https://doi.org/10.1016/S0304-3894(02)00282-0.

Nidheesh, P. V., Ganiyu, S. O., Martínez-Huitle, C. A., Mousset, E., Olvera-Vargas, H., Trellu, C., & Oturan, M. A. (2023). Recent advances in electro-Fenton process and its emerging applications. *Critical Reviews in Environmental Science and Technology, 53(8)*, 887–913. https://doi.org/10.1080/10643389.2022.2093074.

Nouri Sarabi, L., Shariati, S., Islamnezhad, A., & Kefayati, H. (2024). Electro-Fenton process based on sacrificial iron electrode for Ponceau 4R removal. *Water, Air, & Soil Pollution, 235,* 546. https://doi.org/10.1007/s11270-024-07351-7

Olvera Bautista, I., Ocampo Fletes, I., Tornero Campante, M. A., Silva Gómez, S. E., &

González Flores, E. (2021). Calidad agronómica del agua residual tratada utilizada en la producción agrícola en Atlixco, Puebla. *Agricultura, Sociedad y Desarrollo, 17(4),* 603–614. https://doi.org/10.22231/asyd.v17i4.1394.

. Quispe Cardenas, L. E., Deptula, P. J., Huerta, C. S., Zhu, C., Ye, Y., Wang, S., & Yang, Y. (2023). Electro-Fenton and induced electro-Fenton as versatile wastewater treatment processes. *ACS ES&T Engineering, 3(10)*, 1547–1556. https://doi.org/10.1021/acsestengg.3c00128.

Ramos Ascue, J. D. (2018). Online measurement of COD by correlation of the spectral absorption coefficient of UV light. *Producción + Limpia, 13(2)*, 67–76. https://doi.org/10.22507/pml.v13n2a8.

Ribeiro, J. P., & Nunes, M. I. (2021). Recent trends and developments in Fenton processes for industrial wastewater treatment: A critical review. *Environmental Research, 197*, 110957. https://doi.org/10.1016/j.envres.2021.110957

Secretaría de Medio Ambiente y Recursos Naturales (SEMARNAT). (2021). Norma Oficial Mexicana NOM-001-SEMARNAT-2021, que establece los límites máximos permisibles de contaminantes en las descargas de aguas residuales en cuerpos receptores. Diario Oficial de la Federación. Available at: https://www.dof.gob.mx/nota_detalle.php?codigo=5634148&fecha=11/03/2022. Accessed: January 26, 2026.

Silva Gómez, S.E., Muñoz Orozco, A., De la Isla de Bauer, M., Infante Gil, S. (2002). Contaminación ambiental en la región de Atlixco: Agua. *Terra Latinoamericana 20(3)*, 243-251. https://www.redalyc.org/pdf/573/57320303.pdf.

Soto-Vázquez, A., Sánchez-Galindo, P., Barraza-Madrigal, J. A., & Guzmán-Castañeda, J. I. (2023). Electrocoagulation as a possible treatment for wastewater polluted with industrial lubricant oils. *Revista Mexicana de Ingeniería Química, 22(2)*, 1–12. https://doi.org/10.24275/rmiq/IA2313.

Socrates, G. (2004). *Infrared and Raman characteristic group frequencies: Tables and charts.* John Wiley & Sons Editorial, England.

Srinivasa Pilli, S., Yan, S., Tyagi, R. D., & Surampalli, R. Y. (2015). Overview of sludge pretreatment technologies for enhancing anaerobic digestion and dewaterability. *Reviews in Environmental Science and Bio/Technology*, *14(3),* 453–478. https://doi.org/10.1007/s11157-015-9368-4.

Suhan, M. B. K., Shuchi, S. B., Anis, A., Haque, Z., & Islam, M. S. (2020). Comparative degradation study of Remazol Black B dye using electro-coagulation and electro-Fenton process: Kinetics and cost analysis. *Environmental Nanotechnology, Monitoring & Management, 14*, 100335. https://doi.org/10.1016/j.enmm.2020.100335.

Sun, M., Chen, F., Qu, J., Liu, H., & Liu, R. (2015). Optimization and control of electro-Fenton process by pH inflection points. *Chemical Engineering Journal, 269*, 399–408. https://doi.org/10.1016/j.cej.2015.01.115

UNESCO. (2015). The United Nations world water development report 2015: Water for a sustainable world. UNESCO. Available at: https://www.unesco.org/reports/wwdr/2015. Accessed: January 26, 2026.

Vázquez Romero, M., Abril González, M. F., Pinos Vélez, V., García Zumalacarregui, J., Maldonado Carchi, D. D., & Miranda Morales, B. (2024). Fenton process by volcanic ash to eliminate aniline of aqueous solution from the dyeing of toquilla straw crafts. *Revista Mexicana de Ingeniería Química, 23(2),* 1–8. https://doi.org/10.24275/rmiq/Cat24238.

Weishaar, J. L., Aiken, G. R., Bergamaschi, B. A., Fram, M. S., Fujii, R., & Mopper, K. (2003). Evaluation of specific ultraviolet absorbance as an indicator of the chemical composition and reactivity of dissolved organic carbon. *Environmental Science & Technology, 37(20),* 4702–4708. https://doi.org/10.1021/es030360x.

World Health Organization. (2017). Progress on drinking water, sanitation and hygiene. WHO. Available at: https://www.who.int/publications/i/item/9789241512893. Accessed: January 25, 2026.

Wu, Y., Wu, R., Zhou, H., Zeng, G., Kuang, C., Li, C. (2024). Sustainable electro-Fenton simultaneous reduction of Cr(VI) and degradation of organic pollutants via dual-site porous carbon cathode driving uncoordinated molybdenum sites conversion. *Water Research 259*, 121835. https://doi.org/10.1016/j.watres.2024.121835.

Xu, Y., Liu, P., & Zhang, Y. (2022). Mid-infrared spectroscopy of hemispherical water droplets. *Spectrochimica Acta Part A: Molecular and Biomolecular Spectroscopy, 264*, 120256. https://doi.org/10.1016/j.saa.2021.120256.

Yang, R., Wang, H., Zhu, X., Sun, Z. (2025). Review on electrochemical processes for the treatment of heavy metal complexes in wastewater: Performance, mechanism, application and improvement. *International Journal of Electrochemical Science 20(4)*, 100971. https://doi.org/10.1016/j.ijoes.2025.100971.

Ziembowicz, S., Kida, M. (2022). Limitations and future directions of Fenton-like processes. *Chemosphere 296*, 134041. https://doi.org/10.1016/j.chemosphere.2022.134041.

Zhou, Z., Liu, M., Zhang, H., & Sun, D. (2012). Synthesis, characterization and flocculation activity of $Fe(OH)_3$–polyacrylamide hybrid polymer. *Journal of Hazardous Materials, 243*, 41–49. https://doi.org/10.1016/j.jhazmat.2012.10.011.